Population synthesis in galactic nuclei using a library of star clusters [*]

E. Bica

Observatoire de Paris, Section de Meudon, F-92195 Meudon Principal Cedex, France

Summary. Population syntheses for normal nuclei in E/S0 and spiral galaxies are derived using a library of star clusters. This method allows to determine the chemical enrichment and to date successive generations of star formation. Thus it is more than a simple population synthesis, providing for the first time a direct estimate of the chemical evolution in these nuclei. For the E/S0 groups following the normal metallicity vs luminosity relationship, the last generation of stars in the nucleus has reached a metallicity 4 times solar for $M_B = -22$ and 0.5 to 0.3 solar for $M_B = -18$. The bulk of the population is older than 10 Gyr but these galaxies have formed stars at least until look-back times of $\simeq 5$ Gyr. Some metallicity dispersion is detected within the nuclei: in the most metal rich group, around 10% of the optical flux arises from populations with metallicities lower than solar. For the relatively less numerous bluer E/S0 groups, younger age components are present, which we have been able to isolate and date. The red spiral groups also form a metallicity sequence which is related to the bulge luminosity, spanning metallicities from a factor 4 solar to solar. Finally, the groups of bluer spiral nuclei contain younger age components superimposed on an older population, which has reached at least the solar metallicity. The relative importance of the star formation bursts with respect to the older population is derived: in the bluest group, with NGC 5236 as a prototype, the population younger than $3\ 10^8$ yr amounts to 87% of the flux at 4000 Å and 57% at 9000 Å. The present method constitutes a powerful tool for the interpretation of composite spectra and will certainly have many applications in the study of large redshift galaxies.

Key words: galaxies: evolution of – galaxies: stellar content of – galaxies: general – galaxies: nuclei of

1. Introduction

Previous studies of population synthesis in galaxies have been performed with libraries of stellar spectra and, in some cases, with libraries containing a mixture of stars and globular clusters (Pagel and Edmunds, 1981; Pickles, 1985 and references therein). We have undertaken a different approach using a base of *star cluster*

integrated spectra only. A synthesis using stars requires the knowledge of T, g, Z and of the slope of the Initial Mass Funtion (IMF). The latter parameter is implicit in real cluster spectra. Clearly, the advantage of the present method is to be a two parameter analysis: age and metallicity (Bica and Alloin, 1986a, hereafter BA 86a).

We have obtained visible and near-infrared spectra for a large sample of star clusters and galaxy nuclei at 12 Å resolution, respectively with the European Southern Observatory (ESO) telescopes 1.52-m using the Image Dissector Scanner and 2.2-m using a CCD. The visible cluster spectra are discussed in BA 86a while those of galaxy nuclei are presented in Bica and Alloin (1987a, hereafter BA 87a). The near-infrared results are given in Bica and Alloin (1987b, hereafter BA 87b). The sample clusters had a priori known age, metallicity $[Z/Z_\odot]$ and reddening. Thus it has been possible to study the equivalent widths (W) and continuum distribution in the integrated spectra as a function of age and $[Z/Z_\odot]$ (BA 86a). Then a grid of star cluster properties was interpolated at suitable steps in age and $[Z/Z_\odot]$ and the results were given in Bica and Alloin (1986b, hereafter BA 86b) and BA 87b, respectively for the visible and near-infrared ranges.

An important result of this analysis is that the equivalent widths W of metallic lines in the near-infrared are simple functions of $[Z/Z_\odot]$, while those in the blue are sensitive to age, in addition to metallicity, owing to the dilution effect of blue luminous stars in young clusters. The spectra of star clusters and galaxy nuclei had been previously corrected for foreground reddening. The internal reddening arising from inclination effects in spiral galaxies was straightforwardly removed using the method developed in BA 87a. We have also shown that the Na I 5890 Å doublet is not suitable for population synthesis, owing to its interstellar gas contribution, which may dominate the stellar one in the case of inclined spiral galaxies (Bica and Alloin, 1986c, hereafter BA 86c).

The present paper deals with the synthesis results. In Sect. 2 we group the galaxy spectra showing similar properties. In Sect. 3 we present details of the synthesis method and the computations. In Sect. 4 we discuss the synthesis results for our 15 types of galaxy spectra. Section 5 provides comments on the synthesis for individual groups. Finally, the concluding remarks of this work are given in Sect. 6.

2. The spectral groups

Initially we intended to obtain a mean galaxy spectrum for each box determined by morphological type vs luminosity class. Nevertheless it soon became clear that every box contained

Table 1. The galaxy groups

Group	Prototype	Other Galaxies
E1	NGC 4472	NGC 1399, NGC 3557, NGC 3923, NGC 4406, NGC 4486, NGC 4552, NGC 4621, NGC 4649, NGC 5090, NGC 7144, IC 1459
E2	NGC 3115	NGC 1339, NGC 1379, NGC 1387, NGC 1411, NGC 1537, NGC 1574, NGC 1596, *NGC 2434, NGC 3379, NGC 3818, NGC 3904, NGC 4435, NGC 4478, NGC 4958, NGC 7041, NGC 7145
E3	NGC 4033	NGC 1381, NGC 1427, NGC 4976
E4	NGC 4476	NGC 3056
E5	NGC 6861	NGC 584, NGC 1201, NGC 1395, NGC 1404, NGC 1553, NGC 1600, NGC 3585, NGC 4374, NGC 4697, *NGC 4936, *NGC 5266, NGC 5419, NGC 6758, NGC 6776, NGC 7507, NGC 7744, *NGC 6868, IC 4296, IC 4329, IC 4797, IC 4889, IC 5105
E6	NGC 5061	NGC 5018
E7	NGC 2865	NGC 4742, NGC 4382
E8	NGC 5102	
E9	NGC 4486B	NGC 1366, NGC 1400, NGC 4387, NGC 4479
S1	NGC 7049	NGC 524, NGC 1380, NGC 1398, NGC 1533, NGC 4594, NGC 4767, NGC 7329, NGC 7410
S2	NGC 1350	NGC 488, NGC 1316, NGC 1371, NGC 1543, NGC 1617, NGC 4548, NGC 4856, *NGC 5101, NGC 5746, IC 5267
S3	NGC 3521	NGC 289, NGC 692, NGC 779, NGC 1232, NGC 1302, NGC 1425, NGC 1512, NGC 2781, NGC 2811, NGC 3054, NGC 3223, NGC 3358, NGC 3368, NGC 3623, NGC 4192, NGC 4438, NGC 4440, NGC 4462, NGC 4501, NGC 4579, NGC 5064, NGC 5612, NGC 6684, NGC 6744, NGC 6923, NGC 6925, NGC 6942, NGC 7079, NGC 7184
S4	NGC 3887	NGC 772, NGC 908, NGC 1353, NGC 1637, *NGC 2442, NGC 3627, NGC 4254, *NGC 4981, NGC 5121, NGC 5156, NGC 7083, NGC 7205, NGC 7421
S5	NGC 2997	NGC 3351, NGC 4038, NGC 4321, NGC 4536, NGC 5248, NGC 6699, NGC 6782, NGC 7392
S6	NGC 4303	NGC 1084, NGC 4039, NGC 6215, IC 5325
S7	NGC 5236	*NGC 986, NGC 2903, NGC 4027, NGC 4535, NGC 4569, NGC 7552
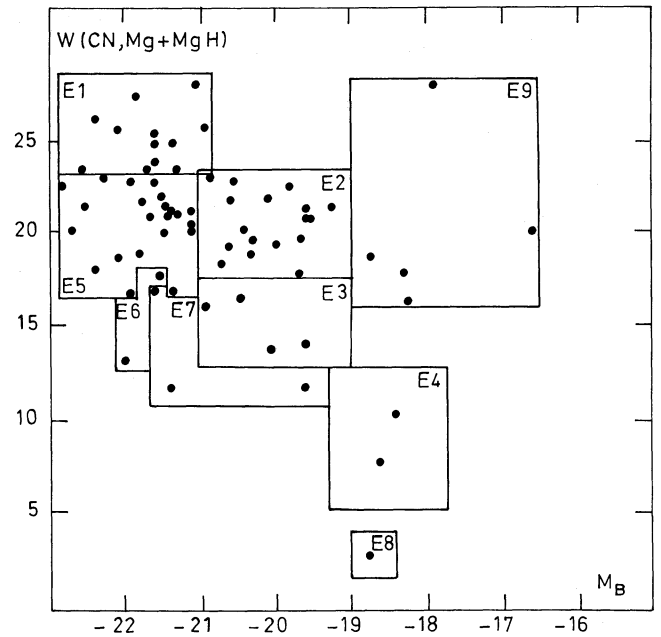
Fig. 1. Distribution of the E/S0 groups in a metal indicator vs absolute magnitude diagram

atypical spectra and particularly that late type spiral galaxies were forming a highly heterogeneous class, for which no prototype could be assigned (BA 87a). Thus we have first grouped spectra sharing the same properties within error bars and in a second step made the further separations according to morphological type or luminosity class. However, we have analyzed E/S0 and spiral galaxies separately. The galaxies in each group are given in Table 1 and values of W and continuum distribution for the various groups are shown in Table 3. The descriptions of the different kinds of spectra, in BA 87a, have delineated the present groups. We obtained nine groups for early-type galaxies (Table 1). They are shown in Fig. 1, in terms of the best metallicity indicator and of the total magnitude M_B. The latter relationship has been discussed in detail in Bica and Alloin (1987c, hereafter BA 87c). Groups El to E 4 correspond to galaxies which follow the normal metallicity

Notes to Table 1:
* In addition to the previous corrections of foreground and spiral inclination reddening (BA 86c, 87a, 87c), it was necessary to apply supplementary corrections for the following galaxies:
NGC 2434 ($E(B-V) = 0.11$): E galaxy at low Galactic latitude. The cosec law value was certainly underestimated.
NGC 2442 (0.29): dust possibly associated with nucleus. Perhaps more inclined than suggested by the axial ratio, which is uncertain owing to asymetric arms. No reddening correction due to inclination was previously applied. Also low Galactic latitude.
NGC 986 (0.17) and NGC 4981 (0.17): possibly internal reddening associated with nucleus.
NGC 5101 (0.07): possibly nuclear internal reddening; strong liner in nearly face-on SBa.
NGC 4936 (0.16) and NGC 6868 (0.09): possibly nuclear internal reddening; strong liners in early-type galaxies.
NGC 5266 (0.15): Early-type galaxy with dust lane along the minor axis. Also low Galactic latitude

Table 2. The distribution of the spiral groups as a function of morphological types and absolute magnitude

	Sa	Sb	Sc
Spectral group S1:			
$M < -22$	1	2	1
$-22 < M < -21$	4	–	–
$M > -21$	1	–	–
Spectral group S2:			
$M < -22$	1	2	–
$-22 < M < -21$	3	1	–
$M > -21$	4	–	–
Spectral group S3:			
$M < -22$	1	2	3
$-22 < M < -21$	5	8	5
$M > -21$	4	2	–
Spectral group S4:			
$M < -22$	–	2	1
$-22 < M < -21$	–	2	3
$M > -21$	1	1	4
Spectral group S5:			
$M < -22$	–	1	1
$-22 < M < -21$	–	–	6
$M > -21$	–	1	–
Spectral group S6:			
$M < -22$	–	–	–
$-22 < M < -21$	–	–	3
$M > -21$	–	–	2
Spectral group S7:			
$M < -22$	–	1	–
$-22 < M < -21$	–	1	4
$M > -21$	–	–	1

absorption lines (Table 3). The component which enhances the Balmer lines could also be responsible for the dilution of metallic lines, which otherwise should be much stronger in such massive galaxies. We emphasize however that the objective of the spectral groups and the subsequent syntheses is not to explore such marginal differences between neighbouring groups. These should be regarded, rather, as the limits for the application of the method.

The selected groups of spiral galaxies are shown as a function of morphological type and luminosity class in Table 2. Notice how the red groups S 1 to S 4 migrate *simultaneously* towards lower luminosities *and* later morphological types. This is indeed a metallicity sequence spanning a factor 4 in metallicity (Sect. 4), which is associated with the bulge size of the galaxies. On average, the nuclear properties of a giant Sc are similar to those of a dwarf Sa. Note that galaxies in the most metal poor groups S 3 and S 4 are strong-lined, very different from metal-poor globular clusters (BA 87a). Groups S 5 to S 7 are subject to various age effects (Sect. 5). The position of these galaxies in the grids of Table 2 gives information on the nature of the older underlying population.

Within each E or S group a small dispersion in spectral properties exists and, in some cases, we have possibly sacrified information for the sake of a better signal to noise ratio. However the quantitative criterium used in the definition of the groups makes the present classification a more detailed and precise version of the early blue-violet spectral types of galaxies (Humason et al., 1956). The extreme groups S 1 and S 7 correspond respectively to the K and A spectral types. We point out that the ranking order E 1–9 and S 1–7 are simple designations not necessarily intended to represent sequences whatsoever. However, the synthesis results (Sects. 4 and 5) indicate that E 1 to E 4 and S 1 to S 3 form, basically, sequences of decreasing average metallicity at constant (mostly old) age population content. On the other hand S 4 to S 7 form a sequence of increasing young age population content at nearly constant average metallicity.

Prior to averaging the spectra, it was necessary to apply a supplementary reddening correction to some particular galaxies, in addition to that arising from foreground sources or spiral inclination effects (Sect. 1). Evidence is found, as noted in Table 1, that for most of these galaxies, the extinction arises from an atypical amount of dust in the nuclear region, but for others at low Galactic latitudes, it possibly arises from uncertainties in the previous foreground reddening correction.

We call attention to the fact that some E and S groups are essentially indistinguishable from a purely spectroscopic viewpoint (Table 3): in particular the strong-lined E 1 group is similar to S 1 and E 2 to S 2. Thus the star formation history of these nuclei must have been very similar, in spite of the fact that the global galaxies differ considerably in appearance. Nevertheless the spiral groups which present clear young age population components (S 5 to S 7, cf. Sect. 4 and 5) are spectroscopically very different from the E 7 and E 8 groups, for which age effects are the strongest among early-type galaxies. This suggests, at least for the present sample, that whenever star formation has occured in the nuclei after the initial collapse, it has been different in spirals and ellipticals.

3. Principle of the method and computations

We have used for the computations strong metallic features over a *wide spectral range*. Metallic lines provide constraints on the metal content; but they also constitute a powerful age discriminator owing to their W wavelength dependence, which arises from

vs luminosity relationship, being dominated by a very old stellar population. Groups E 5 to E 8 mostly show age effects, as discussed in Sect. 4. The shapes of the boxes in Fig. 1 are rather irregular: they reflect the fact that the consideration of only two metallic lines is in general insufficient to determine all spectral properties. This is illustrated particularly by a comparison of E 3 and E 7 which have similar W(CN) and W(MgI) but differ considerably in terms of W(Hβ) and other Balmer lines, as well as in terms of continuum distribution (Table 3 and Figs. 4 and 8). Thus we have also taken into account the latter important spectral properties in the definition of our groups. Group E 9 corresponds mostly to galaxies with an evidence of tidal stripping (BA 87c and references therein). However, spectroscopically it is indistinguishable from group E 2, which indicates that the star formation took place quite early, before the stripping. Owing to their similar properties we synthesize only the group E 2. Group E 2 is also spectroscopically very similar to the more luminous E 5, but we have decided to keep them apart because there is no evidence that E 2 are simply stripped E 5 galaxies. Rather, E 5 might have been very strong-lined like E 1 and the spectral similarity with E 2 should arise from an additional population component which dilutes the metallic lines. E 3 and E 6 are, perhaps, a more clear example of this effect: at similar metal indicator value (Fig. 1), the more luminous group E 6 presents a systematic increase of Balmer

Table 3. Observed and computed properties and determination of the nuclear reddening

Group	W(K) 3933	W(CN) 4200	W(G) 4301	W(Mg I) 5175	W(Ca II) 8542	8662	Hβ 4861	Hγ 4340	Hδ 4102	Cont 4020	Cont 4570	Cont 7520	Cont 8700	E(B−V) nucl.
E1	16.8	14.5	9.3	10.3	6.1	4.9	3.4	4.8	5.7	0.48	0.81	0.99	1.02	0.04
Temp.	18.7	15.0	10.3	9.2	6.4	5.7	3.8	5.1	4.8	0.49	0.76	0.98	0.99	
E2	17.2	10.9	9.2	9.5	6.2	5.3	3.6	5.1	4.9	0.53	0.82	1.00	1.01	0.05
Temp.	17.8	13.3	9.7	8.3	5.7	5.3	3.7	5.0	5.8	0.53	0.78	0.97	0.97	
E3	15.3	7.3	8.6	7.7	6.6	5.5	3.4	3.8	2.0	0.57	0.85	0.98	0.96	0.01
Temp.	14.9	9.4	8.2	6.3	5.0	4.6	3.6	4.9	4.4	0.60	0.81	0.94	0.92	
E4	13.7	3.4	6.8	6.3	5.2	4.7	ec	4.6	3.8	0.61	0.88	0.92	0.90	0.05
Temp.	12.0	5.7	6.5	5.5	4.4	3.9	3.7	4.6	4.6	0.65	0.84	0.92	0.89	
E5	15.8	10.6	8.7	9.6	5.4	4.5	3.4	4.0	3.8	0.50	0.81	1.00	0.99	0.05
Temp.	17.9	14.1	9.9	8.9	6.2	5.6	3.5	5.2	5.2	0.54	0.79	0.97	0.97	
E6	14.0	7.9	8.3	7.4	5.7	5.3	4.4	4.9	3.9	0.56	0.86	0.96	0.95	0.05
Temp.	15.5	10.9	8.5	7.2	5.3	4.9	4.1	5.3	5.1	0.65	0.84	0.93	0.91	
E7	12.5	6.2	6.5	7.2	5.5	5.0	4.7	4.9	5.6	0.67	0.95	0.86	0.83	0.01
Temp.	13.5	9.5	7.4	6.6	5.3	4.9	4.9	6.1	6.8	0.76	0.91	0.90	0.86	
E8	6.4	0.3	2.5	2.6	4.6	3.9	ec	6.6	9.2	1.21	1.19	0.79	0.72	0.04
Temp.	6.5	2.2	3.2	3.3	4.4	4.0	6.5	7.3	9.5	1.34	1.26	0.77	0.67	
S1	19.0	13.0	10.0	9.8	5.6	4.6	3.6	5.6	5.3	0.47	0.76	1.03	1.03	0.05
Temp.	18.6	14.7	10.2	9.0	6.3	5.6	3.7	5.1	4.6	0.50	0.77	0.98	0.99	
S2	16.4	10.4	8.8	9.2	5.9	4.6	3.7	3.9	4.1	0.50	0.79	1.00	1.02	0.05
Temp.	17.2	12.8	9.5	8.0	5.6	5.2	3.8	5.1	4.7	0.55	0.79	0.96	0.96	
S3	15.5	8.5	8.5	7.9	5.7	4.6	3.8	4.4	3.1	0.56	0.85	0.95	0.92	0.02
Temp.	15.3	10.8	8.5	7.1	5.3	4.9	3.9	5.2	4.9	0.61	0.82	0.94	0.92	
S4	13.1	6.2	7.3	6.3	6.2	4.7	4.2	5.4	4.2	0.59	0.80	1.02	0.98	0.04
Temp.	13.3	9.0	7.5	6.3	5.2	4.7	4.0	5.3	5.1	0.68	0.86	0.93	0.90	
S5	6.4	4.6	5.5	6.2	4.8	5.4	ec	ec	ec	0.67	0.87	0.98	0.94	0.07
Temp.	9.9	6.6	5.9	5.2	4.7	4.3	3.6	4.7	4.5	0.80	0.91	0.91	0.87	
S6	5.5	3.9	4.6	3.7	—	—	ec	ec	ec	0.86	0.95	0.95	—	0.06
Temp.	8.1	5.5	4.9	4.8	4.7	4.3	3.8	4.9	4.9	0.94	0.99	0.89	0.84	
S7	3.5	2.4	2.2	3.3	5.4	5.4	ec	ec	ec	1.34	1.27	0.76	0.63	0.01
Temp.	4.5	3.0	2.1	3.2	4.8	4.4	5.4	6.5	7.2	1.53	1.31	0.78	0.68	

Note to Table 3:
ec means that all galaxies in the group have the corresponding Balmer line contaminated by emission. Whenever part of the galaxies are contaminated, these were excluded from the mean

dilution by blue stars in young star clusters (BA 86a). We use K Ca II 3933 Å, CN 4200 Å, the G band of CH 4301 Å, Mg I + MgH 5175 Å and Ca II 8542, 8662 Å. These are strong features measured with a good precision, they are not disturbed by emission lines and have a comprehensively-modeled behaviour as a function of the cluster age and metallicity (BA 86b, 87b). The Na I 5890 Å line is strong as well, but the interstellar contamination precludes its use for population synthesis (BA 86c). Red TiO bands are not used owing to their complex behaviour in young clusters containing luminous red stars; this behaviour has to be further studied (BA 86a, 87b) before we can model it. However, we use the TiO bands to check the output of the computations, since the resulting template galaxy spectrum, built from a combination of star cluster spectra, must reproduce them as well. The Balmer lines can be used only when they are free of emission contributions: Hα, as a

rule, is emission contaminated, even when seen in absorption. In the latter case however, Hβ can be safely employed and so on for Hγ and Hδ. For the spiral groups S 5 to S 7, all Balmer lines are contaminated, so the computations in these cases rely exclusively on metallic features.

Previous population syntheses have used, in general, minimization procedures which looked for the best solution, starting from a plausible initial guess. The problem in these computations has always been to test the uniqueness of the solution. This has been very difficult, if not impossible altogether, owing to the fact that many parameters can be modified in a synthesis using stellar libraries.

Using a fast computer and having only two parameters, age and metallicity, it has been possible to test an extremely large number of star cluster combinations, and thus to be more

confident about the uniqueness of the solution we found. Two chemical evolution arguments constrain the space in the $[Z/Z_\odot]$ vs age plane where the solution is searched for. First, galaxy nuclei correspond to small volumes where it is plausible to assume that the gas is chemically homogeneous at any time, so that the solution must describe a path in the diagram. Second, the metallicity cannot decrease for younger generations. Thus in a first phase, the method consists of testing all possible combinations at 10% step of 8 points (clusters) which form a path (chemical evolution) in the age versus $[Z/Z_\odot]$ plane. We point out that it is not possible to have time information for ages older than ~ 8 Gyr. We assume in this work that the chemical enrichment in the nuclei has taken place quite early. Thus in practice an initial path of 8 star clusters in the $[Z/Z_\odot]$ vs age diagram is distributed along two sequences: (i) a metallicity sequence from $[Z/Z_\odot] = -2$ to $[Z/Z_\odot]_{max}$ at fixed very old age and (ii) an age sequence down to 10^6 yr at constant $[Z/Z_\odot]_{max}$ (see Tables 4 and 5). Typically we test 5 paths which reach up respectively $[Z/Z_\odot]_{max} = +0.6; +0.3; 0; -0.5$ and -1. We emphasize that the objective is not simply to determine the maximum metallicity reached up by the nucleus, but rather to determine the relative contributions of the different types of clusters along the path. In spite of the fact that it is assumed that all the chemical enrichment has taken place in the old age bin, the relative contributions of the components of differing metallicity in this bin, still tell us about the chemical evolution (e.g. Hartwick, 1976). The points along the path are taken from the grid of cluster properties which was interpolated at suitable steps in age and metallicity (BA 86b, 87b). The program selects the solutions which reproduce the galaxy W values within the error bars. Typically those error bars are windows amounting to 10% of a given galaxy W value. We recall that for 8 points (clusters) at 10% step, 19448 combinations have a sum of individual contributions totalling 100%. The result consists of 5–20 solutions which form a highly degenerate family in the sense that a cluster contribution in the set of solutions in general does not vary by an amount larger than the 10% step. The ratio between the number of solutions found with respect to the total number of tested combinations in the 5 paths provides an estimate of the uniqueness of the result. We find that a typical family of solutions corresponds to 1 part among 10000 possibilities.

A second phase consists of exploring at a 5% step, a restricted space of combinations centred on the family of solutions found during the first phase. This time we use a larger number of points (clusters) in the grid path and we obtain a larger number of degenerate solutions. This allows to make statistics on the individual cluster contributions. Thus a small star cluster contribution of 1% in Tables 4 and 5 means that on average one solution presents a 5% contribution and in four others it results null. In the second phase the solutions remain essentially the same, but the finer star cluster step then employed quite often provides improvements in the sense of an astrophysically more plausible solution such as more smoothly increasing contributions towards high metallicities in the old age bin.

Another way of estimating the uniqueness of the solution and the relevance of the small number contributions in Tables 4 and 5 is to compare the outcome for groups with similar input spectra and to analyze the path obtained and the corresponding contributions of the three main components: (i) old metal rich; (ii) old metal poor and (iii) young component. We conclude that the relevance of differences in synthesis results between e.g. E 5 and E 2 are marginal, whereas e.g. between E 6 and E 3 are significant. In fact for part of the E groups the family of solutions is distributed between two metallicity paths and we have adopted the

one where other E groups with similar luminosity occured. Thus E 5 was placed in a path reaching the same metallicity as E 1, and E 6 was matched to E 2 in order to compare the resulting models assuming equal upper metallicity. On the other hand differences between non-neighbouring groups like e.g. E 1 and E 3 are fully significant. We also conclude that the contributions become relevant at the 10% level; however the small numbers accessed statiscally should not be disregarded. Although higher precision is always desirable, we do not think it will considerably improve the situation. Rather, it is the addition of information in other spectral regions like the near-ultraviolet that will help to constrain more the models. In the present work if only the visible range were available not much information would have been extracted from the data because we have verified that the near-infrared Ca II lines have been fundamental for separating the competing contributions from old metal poor and young components.

It is important to note that no constraints are imposed on the continuum distribution. Instead the resulting continuum when compared to that of its respective real galaxy group is used to determine the nuclear reddening.

4. Results and discussion

The mean observed W values for each galaxy group are given in Table 3 together with those for the computed templates. A set of observed and calculated continuum points are also shown, from which we derived a nuclear reddening $E(B-V) \cong 0.04$ affecting most groups. We emphasize that the W computations straightforwardly give this kind of solution for the continuum distribution. The fact that we obtain neither solutions with an awkward continuum distribution nor solutions demanding a negative reddening correction is evidence that the library of clusters and the spectral range spanned by our observations have considerably constrained the synthesis problem. We interpret the resulting $E(B-V) \cong 0.04$ as a global extinction present in the bulge of many galaxies. A doubt could remain whether this extinction arose from an underestimation of the reddening in our Galaxy, since we have used foreground corrections according to Sandage and Tammann (1981), who predict very low Galactic reddening. However Sparks et al. (1987) find independent evidence favouring this low reddening model, using Balmer-line flux ratios in H II galaxies. We have also compared the cosec law values adopted in this paper with the values from Burstein and Heiles (1984), which are based on H I column densities and galaxy counts. Nearly 75% of the present sample are high Galactic latitude galaxies and both methods predict $E(B-V) < 0.04$ with essentially no zero-point systematic difference. For the rest of the sample Burstein and Heiles' method predicts on average slightly stronger reddening values. Thus in the groups of Table 1 a large systematic difference arising from foreground reddening corrections is not probable. Consequently we conclude that our excess of reddening $E(B-V) \cong 0.04$ arises indeed from a small amount of dust present in the interstellar medium of central regions of all galaxies, even in the absence of obvious evidence of recent star formation. We also call attention to the fact that we have not applied internal reddening corrections to our library of star clusters. Thus the computations make use of blue cluster and H II region continua affected by the extinctions which are inherent to star forming regions. This procedure is justified because in the case of galaxy nucleus with regions of recent star formation, the associated dust will certainly be localized within these regions, not necessarily affecting much the surrounding older populations.

Table 4a–h. Percentage contributions at $\lambda = 5870$ Å: the chemical evolution for E/S0 groups

Table 4a
Group E1:

	Age (yr)							
$[Z/Z_\odot]$		RHII	E7	5E7	E8	5E8	E9	5E9	Glob.
	+0.6						3	8	66
	+0.3								9
	0								5
	−0.5								3
	−1.0								3
	−1.5								2
	−2.0								1

Table 4d
Group E4:

	Age (yr)							
$[Z/Z_\odot]$		RHII	E7	5E7	E8	5E8	E9	5E9	Glob.
	+0.6								
	+0.3								
	0								
	−0.5						2	4	55
	−1.0								25
	−1.5								11
	−2.0								3

Table 4b
Group E2:

	Age (yr)							
$[Z/Z_\odot]$		RHII	E7	5E7	E8	5E8	E9	5E9	Glob.
	+0.6								
	+0.3							11	74
	0								6
	−0.5								4
	−1.0								3
	−1.5								1
	−2.0								1

Table 4e
Group E5:

	Age (yr)							
$[Z/Z_\odot]$		RHII	E7	5E7	E8	5E8	E9	5E9	Glob.
	+0.6						3	14	50
	+0.3								14
	0								6
	−0.5								4
	−1.0								4
	−1.5								3
	−2.0								2

Table 4c
Group E3:

	Age (yr)							
$[Z/Z_\odot]$		RHII	E7	5E7	E8	5E8	E9	5E9	Glob.
	+0.6								
	+0.3								
	0							5	64
	−0.5								14
	−1.0								11
	−1.5								4
	−2.0								2

Table 4f
Group E6:

	Age (yr)							
$[Z/Z_\odot]$		RHII	E7	5E7	E8	5E8	E9	5E9	Glob.
	+0.6								
	+0.3						7	17	40
	0								10
	−0.5								9
	−1.0								7
	−1.5								6
	−2.0								4

We present in Tables 4 and 5, respectively for the E/S0 and spiral groups, the resulting percentage contributions at $\lambda = 5870$ Å of the grid points (clusters) of different ages and metallicities. It can be seen that the present method is more than a simple population synthesis, providing for the first time a direct estimate of the chemical evolution of these nuclei. The fact that solutions exist for at least one of the paths in Sect. 3 supports the validity of the assumption that for all groups the chemical enrichment has taken place very early. We can definetely exclude paths in the $[Z/Z_\odot]$ vs age diagram linking a metal poor population directly to a metal rich one younger than 1 Gyr, because these two types of population are too blue, and even our bluest nuclei demand at least some contribution from a red population. We cannot exclude however the possibility that in some groups a metallicity increase of 0.5 has occurred in between the most metal rich globular-like population and that at 5 Gyr. Some enrichment is also possible for ages smaller than 1 Gyr, but this effect would be very hard to detect from the stellar population only, because the integrated spectrum becomes little sensitive to metallicity, particularly for $\lambda < 6000$ Å, owing to the dilution effects of blue stars. For some

Table 4g
Group E7:

$[Z/Z_\odot]$	RHII	E7	5E7	E8	5E8	E9	5E9	Glob.
+0.6								
+0.3				3	5	18	5	33
0								10
−0.5								8
−1.0								7
−1.5								6
−2.0								5

Table 4h
Group E8:

$[Z/Z_\odot]$	RHII	E7	5E7	E8	5E8	E9	5E9	Glob.
+0.6								
+0.3								
0								
−0.5	2	7	6	5	56	2	1	11
−1.0								6
−1.5								3
−2.0								1

Table 5a–g. Percentage contributions at $\lambda = 5870$ Å: the chemical evolution for spiral groups

Table 5a
Group S1:

$[Z/Z_\odot]$	RHII	E7	5E7	E8	5E8	E9	5E9	Glob.
+0.6						1	11	55
+0.3								14
0								9
−0.5								4
−1.0								3
−1.5								2
−2.0								1

Table 5b
Group S2:

$[Z/Z_\odot]$	RHII	E7	5E7	E8	5E8	E9	5E9	Glob.
+0.6								
+0.3						2	10	69
0								7
−0.5								5
−1.0								3
−1.5								2
−2.0								2

Table 5c
Group S3:

$[Z/Z_\odot]$	RHII	E7	5E7	E8	5E8	E9	5E9	Glob.
+0.6								
+0.3						6	8	51
0								9
−0.5								8
−1.0								7
−1.5								6
−2.0								5

Table 5d
Group S4:

$[Z/Z_\odot]$	RHII	E7	5E7	E8	5E8	E9	5E9	Glob.
+0.6								
+0.3								
0	1	1	1	2	1	3	9	65
−0.5								7
−1.0								5
−1.5								3
−2.0								2

groups in Tables 4 and 5, the maximum metallicity is certainly intermediate between two $[Z/Z_\odot]$ values in the grid, because the family of solutions is distributed in two different paths. Thus groups E 2 and S 2 have possibly reached $[Z/Z_\odot] = 0.4$, groups E 3 and S 4 $[Z/Z_\odot] = 0.1$ and group E 4 $[Z/Z_\odot] = -0.3$. A detailed comparison of the nuclear flux contributions at 5870 Å (Tables 4 and 5) with chemical evolution models would require transforming them into mass contributions, as well as taking into account slit projection effects which integrate along the line of sight outer metal poor shells. In the present paper we only point out that the computations indicate a dispersion in metallicity for the observed nuclei (Tables 4 and 5).

We illustrate in Figs. 2–16, for each galaxy group, the real mean galaxy spectrum corrected for the nuclear reddening derived in Table 3 as well as the template galaxy with its decomposition in terms of cluster contributions. We also give the residual spectrum

Table 5e
Group S5:

		Age (yr)						
		RHII	E7	5E7	E8	5E8	E9	5E9	Glob.
	+0.6								
	+0.3								
	0	6	2	2	2	1	2	4	51
$[Z/Z_\odot]$	−0.5								12
	−1.0								7
	−1.5								6
	−2.0								5

Table 5f
Group S6:

		Age (yr)						
		RHII	E7	5E7	E8	5E8	E9	5E9	Glob.
	+0.6								
	+0.3								
	0	9	3	5	5	2	2	4	45
$[Z/Z_\odot]$	−0.5								11
	−1.0								6
	−1.5								5
	−2.0								3

Table 5g
Group S7:

		Age (yr)						
		RHII	E7	5E7	E8	5E8	E9	5E9	Glob.
	+0.6								
	+0.3								
	0	12	10	11	32	7	2	3	17
$[Z/Z_\odot]$	−0.5								2
	−1.0								2
	−1.5								1
	−2.0								1

(galaxy − template) which brings forth the galaxy emission lines as well. Figures 2–16 allow to compare the average emission lines in normal galaxies with the respective underlying population. Most of the galaxies in our sample have very weak or otherwise undetected emission lines. Thus, the mean emission line spectrum for each group corresponds to a phenomenon on a smaller scale than that occuring in typical LINERS (e. g. Keel, 1983). A detailed analysis of the spectrum for each group as well as that of individual strong LINERS, will be presented in a forthcoming paper. In the present work we have excluded 10 galaxies from our initial sample of 164 objects (BA 87a). These are two H II region

nuclei for which the absorption line population is essentially absent and 8 Seyfert or Seyfert-like objects for which a non-thermal continuum contribution is certainly important. For modelling the groups in Table 1 a featureless H II region continuum was considered which was derived from the mean of several extragalactic H II region observations (BA 86a, 87a, 87b). In the computations this component acts only as a dilution agent of metallic features. In the particular case of groups with LINER characteristics this contribution results null and we do not think that an additional non-thermal continuum is detectable, unless it is much steeper than an H II region continuum. This should be further checked with spectra in the near-ultraviolet range.

The star cluster groups used in the decomposition of Figs. 2–16 are averages of spectra from BA 86a and BA 87b. The mean metallicities of the five globular cluster groups are $[Z/Z_\odot] = -1.9$, −1.5, −1.0, −0.4 and +0.05. The latter group consists of the strong-lined inner bulge globular clusters (IBGC), NGC 6440, 6528, and 6553. Note that we have used $E(B-V) = 1.25$ for NGC 6440, the value adopted in BA 86a being slightly underestimated. For the intermediate and young age groups we have used averages of Galactic disc and Large Magellanic Cloud (LMC) clusters, for the sake of a better S/N. This is a reasonable choice because metallicity effects on an integrated spectrum become increasingly smaller towards younger ages. Nevertheless we have excluded the Small Magellanic Clouds (SMC) clusters from these means.

We emphasize that Fig. 2–16 are simply a visualization of the results, using the nearest available clusters, whilst the contributions in Tables 4 and 5 were computed as decribed in Sect. 3, using a detailed grid of cluster properties at suitable steps in age and metallicity. This grid contains a straightforward extrapolation of the cluster properties to $[Z/Z_\odot] = 0.6$ (BA 86b, BA 87b). Particularly, the E 1 galaxy group computations have required the use of grid points at $[Z/Z_\odot] = +0.6$. For its visualization in Fig. 2b we have replaced the 66% contribution of the super metal-rich globular cluster (SMRGC) at $[Z/Z_\odot] = 0.6$ by the observed IBGC group. The strongest residuals in Fig. 2c correspond to the Swan bands with heads at 4737 Å and 5165 Å. The latter region also contains MgH, but the fact that the $(1,0) C_2$ 4737 Å head is clearly identified, implies that a non-negligible amount of absorption from 5000 to 5165 Å is due to the stronger $(0,0) C_2$ head. Indeed, synthetic spectra of stellar types which are expected to dominate the flux in this spectral range predict in many cases C_2 contributions which are stronger than those of MgH (Barbuy, private communication, 1987). The remaining features cancel out quite well, particularly the near-infrared TiO bands. Thus C_2 is very sensitive to an increase in the global metal content from solar to $[Z/Z_\odot] = +0.6$. This strong metallic dependence might be associated with the diatomic nature of the molecule. The C_2 residuals decrease for the galaxy groups which reach $[Z/Z_\odot] = +0.3$ or solar metallicity (e.g. Figs. 3 and 4). Carbon stars do not seem to be responsible for the C_2 residuals, because these stars are very weak in the blue. A suitable number of such stars to explain the C_2 residuals would produce far too much flux in the near-infrared range.

In the strong-lined E and S0 galaxy nuclei significant Na I D residuals also remain. These residuals are possibly associated with an interstellar gas component (BA 86c). The existence of gas, at least in ionized form, is indicated by the emission lines (e.g. Fig. 2). In addition, dust is detected on CCD images for ~25% of elliptical galaxies (Sparks et al., 1985). This dust could also be responsible for the nuclear reddening $E(B-V) \cong 0.04$ derived in the present synthesis (Table 3). In the case of the spiral galaxies,
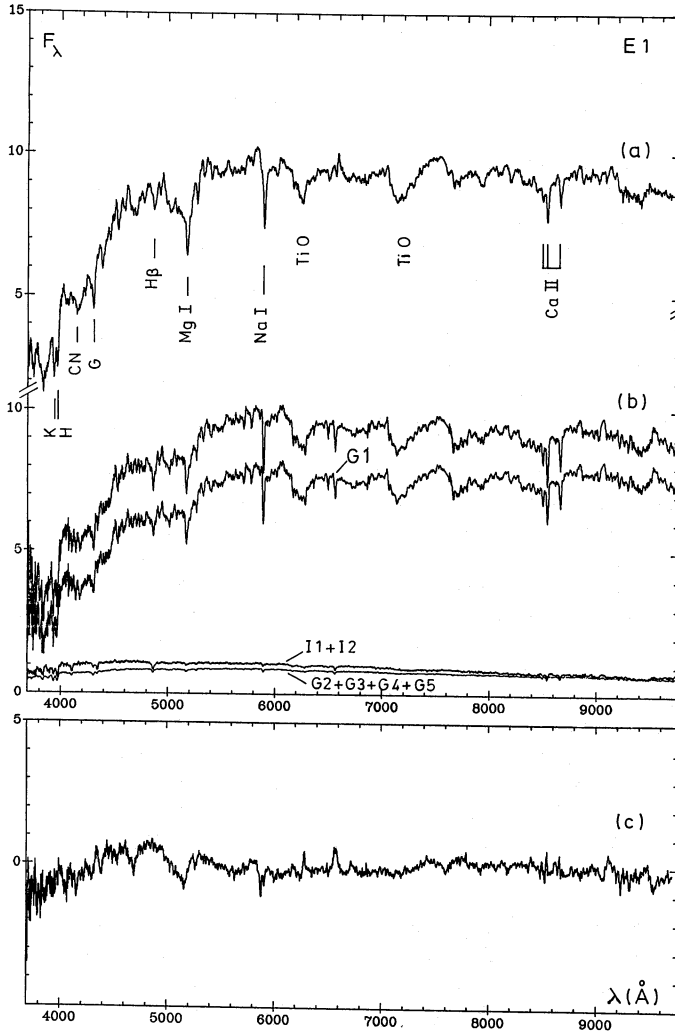
Figs. 2–16. **a** The observed group spectrum; **b** the template built from cluster spectra and its decomposition into individual clusters of differing age and metallicity; **c** residuals and galaxy emission lines. The identifications of the main lines and molecular bands are given in Fig. 2 and 16, respectively for typical red and blue populations. The star cluster groups used for the decomposition in **b** are as follows. Globular clusters: $G1$ ($[Z/Z_\odot] > 0$); $G2$ ($[Z/Z_\odot] = -0.4$); $G3$ ($[Z/Z_\odot] = -1.0$); $G4$ ($[Z/Z_\odot] = -1.5$); $G5$ ($[Z/Z_\odot] = -1.9$). Intermediate age: $I1$ (10^9 yr); $I2$ ($5\ 10^9$ yr). Young clusters: $Y1$ (10^7 yr); $Y2$ ($5\ 10^7$ yr); $Y3$ (10^8 yr); $Y4$ ($5\ 10^8$ yr). H II region: H
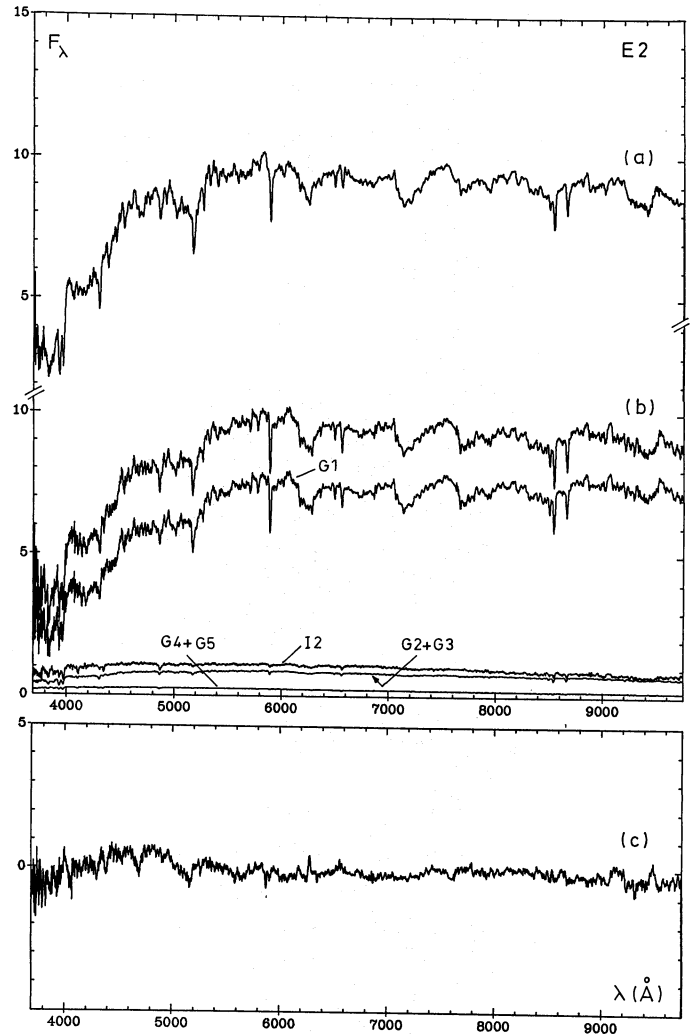
Na I D residuals also show up. But then, they arise at least in part from gas in the disc, because the sample contains many very inclined spiral galaxies (BA 86c).

The spectrum of a SMRGC at $[Z/Z_\odot] = +0.6$ can be empirically derived by subtracting from the galaxy group E 1, all other cluster contributions (Table 4a), as well as the emission line residuals (Fig. 2). This predicted spectrum is compared in Fig. 17 to the observed group IBGC and to the one at $[Z/Z_\odot] = -0.4$. We recall that the object with weakest lines in the latter group is NGC 104 (47 TUC). Thus, this figure shows that the present synthesis was made possible because we have observed the IBGC NGC 6440, 6528 and 6553, which have metallic features almost similar to those in giant galaxies, while star clusters usually called metal-rich in the literature, like 47 TUC, NGC 6637 (M 69), NGC 6838 (M 71) and NGC 6356, would clearly not be suitable. The predicted SMRGC at $[Z/Z_\odot] = +0.6$ will be important for comparisons with synthetic spectra or with clusters in the very center of M 31. It could also be injected in spectral synthesis

models. Indeed its use in other galaxy groups such as S 1, which also requires grid points at $[Z/Z_\odot] = +0.6$, would obviously eliminate the C_2 residuals.

The present synthesis method relies on the assumption that the Initial Mass Function (IMF) within a galaxy nucleus can be reproduced from a combination of the IMF within individual star clusters. There are several sources of uncertainty, such as possible dependences of the IMF on the metallicity and on the kinematics of the initial gas cloud, as well as changes in the luminosity function of the resulting stellar system, as a consequence of dynamical evolution. However, the fact that we obtain satisfactory synthesis results favours the validity of our assumption. Indeed the shape of the IMF in the high mass range, taken over scales $\geqq 1$ kpc appears to be universal, with no compelling evidence for any systematic slope variations depending on metallicity, galactocentric distance or galaxy morphology (Scalo, 1986). On the other hand there is evidence that in its low-mass end, the IMF presents a trend with metallicity, as indicated by the main sequence luminosity function
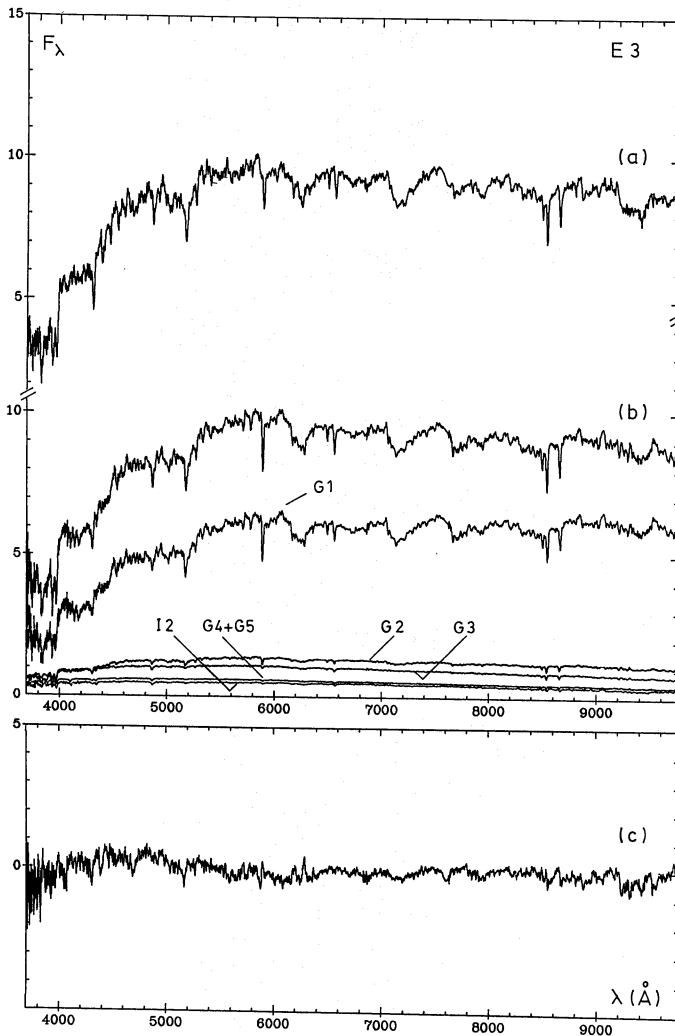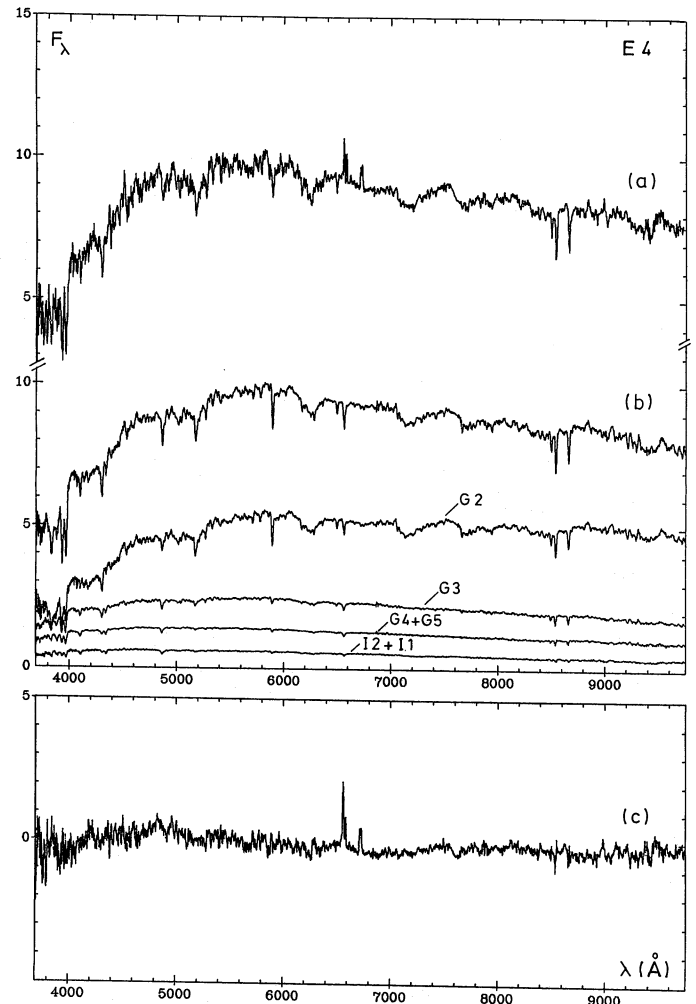
Fig. 4

Fig. 5

of globular clusters from CCD observations (McClure et al., 1986). This dependence is implicitly taken into account in our synthesis, since we use real clusters spanning a wide range of metallicites. Another important question is a possible spatial dependence of the IMF, arising from the initial physical conditions in central regions of galaxies, such as the gas kinematics and a large gas density in a strong gravitational potential. Even star formation in such an environment has possibly been taken into account in our synthesis, because, according to the computations, the dominant type of population in most nuclei, resembles that of the very metal-rich globular clusters NGC 6440, 6528, and 6553. These *are inner bulge objects* which have been formed in such extreme physical conditions. A more difficult problem to solve is the possible effect of the internal dynamical relaxation of star clusters with the subsequent evaporation of low mass stars by tidal effects. However, the main sequence luminosity functions at least in the observed intervals, indicate that the loss of low mass stars occurs only in small clusters (Mc Clure et al., 1986). This effect is minimized in our sample because we have observed the richest clusters in the Galaxy and Magellanic Clouds (BA 86a). The dynamical evolution of galaxy nuclei would be an additional complication. Nevertheless, the satisfactory synthesis results

obtained with our method which does not make an explicit use of the IMF, suggest that in past stellar synthesis, the importance of the slope of the IMF has been, perhaps, overestimated with respect to more interesting parameters like age and metallicity.

Finally we emphasize that the present synthesis method is little dependent on the adopted age and metallicity calibrations for the star clusters. It rather relies upon the properties directly observed in the cluster spectra. Thus, if revisions of the cluster ages and metallicities eventually occur in the future, the proportions of different types of clusters derived in the synthesis will not be affected, only their assigned age and metallicity would have to be modified. It should be stressed that there is still some uncertainty in the high metallicity end of the calibration and that metal abundance determinations of individual stars in the very strong-lined globular clusters NGC 6440, 6528 and 6553 are of great interest.

5. Comments on the synthesis for each group

Groups E 1 to E 4 follow the metallicity vs luminosity relationship (Sect. 2). The results in Tables 4a to 4d together with Fig. 1
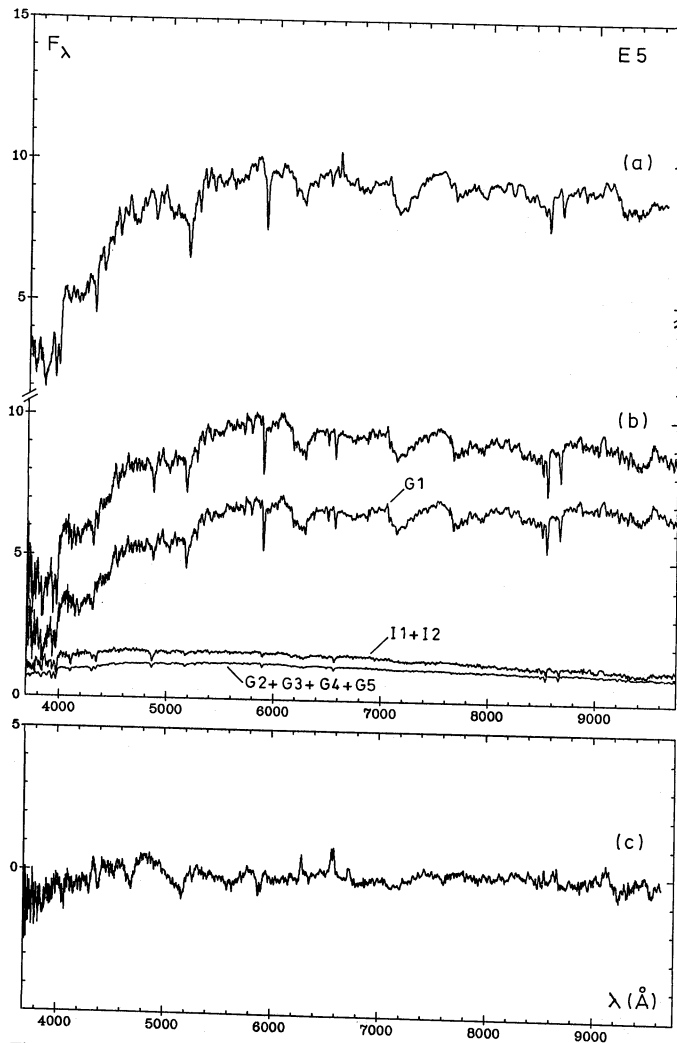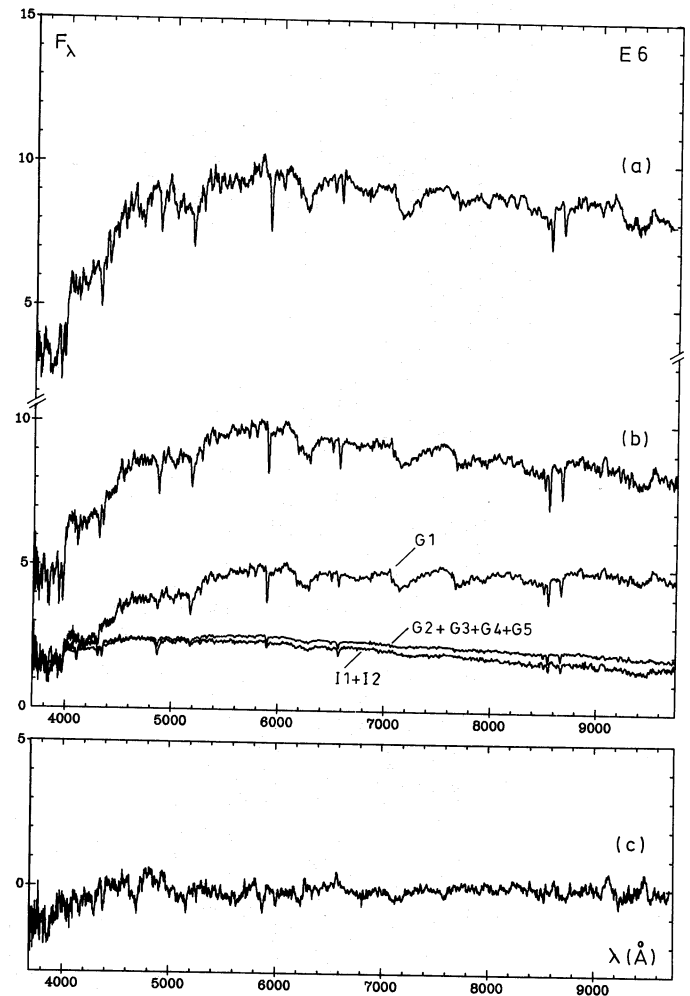
Fig. 6

Fig. 7

indicate that the last generation of stars has reached $[Z/Z_\odot] = +0.6$ at $M_B = -22$ to $[Z/Z_\odot] = -0.3$ or -0.5 at $M_B \cong -18$. The bulk of the population is older than 10 Gyr.

No age has been assigned to the last column of the grids in Tables 4 and 5; we simply call it GC (globular cluster) because the properties of the integrated spectra remain essentially constant for $t \geq 10$ Gyr. However the cluster properties around 5 Gyr are significantly different (Bica, Alloin 86b). The present computations indicate that for the E 1 to E 4 groups this intermediate age population amounts to $\sim 10\%$ in the optical spectrum (Figs. 2–5). No significant contribution from young populations ($T \leq 5\ 10^8$ yr) are detected from the optical data only. Old metal-poor contributions are present even in the strong-lined E 1 group; then the lower than solar metallicity population amounts to 10% in the optical flux (Fig. 2). For the group E 3 the $[Z/Z_\odot] < 0$ population amounts to 30%. Finally, for the group E 4, the whole population is metal-poor.

An extension of the present method to the ultraviolet range, has demonstrated that the UV rising branch in giant elliptical galaxies arises from on-going star formation at a small rate rather than from metal poor populations (Bica and Alloin, 1987d). The

contribution of this very young component has a minor effect in the optical, where at $\lambda = 5870$ Å, it is less than 2%.

The group E 5 contains two types of nuclei (BA 87c): firstly, more distant galaxies which may differ from the strong-lined E 1 galaxies due to an aperture effect bringing a larger contribution from metal-poor components outside the nucleus; secondly, in galaxies for which the slit corresponds to the same volume as that observed for E 1, the spectral difference with respect to E 1 could arise from an age effect. However the differences between the two E 5 subgroups are only marginal, so it is their mean which we have synthesized. The results suggest a slight enhancement of the intermediate age and of the metal-poor components with respect to those in the E 1 group (Table 4e, Fig. 6).

Groups E 6 and E 7 are less constrained in terms of computations. A significant contribution from intermediate age populations is required, particularly for the E 7 group (Table 4g, Fig. 8); but some metal-poor population excess shows up too, with respect to the groups E 1 and E 2. Basically two mechanisms are possible; either a major star formation event which has evolved into an intermediate age population or a merging with a metal-poor galaxy such as those in group E 4, or both. In order to clarify
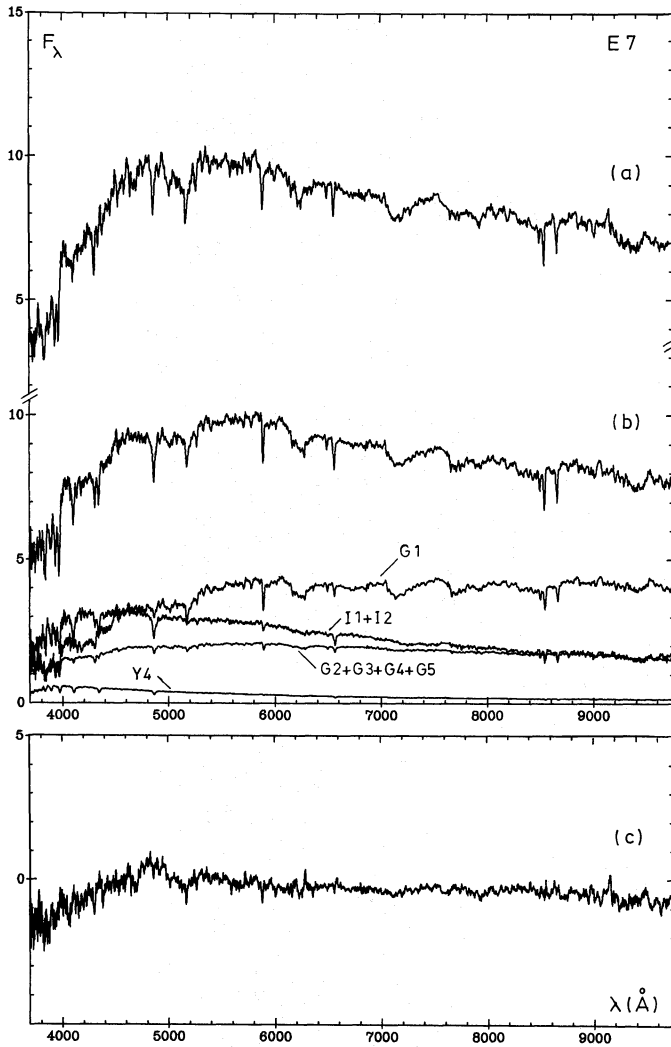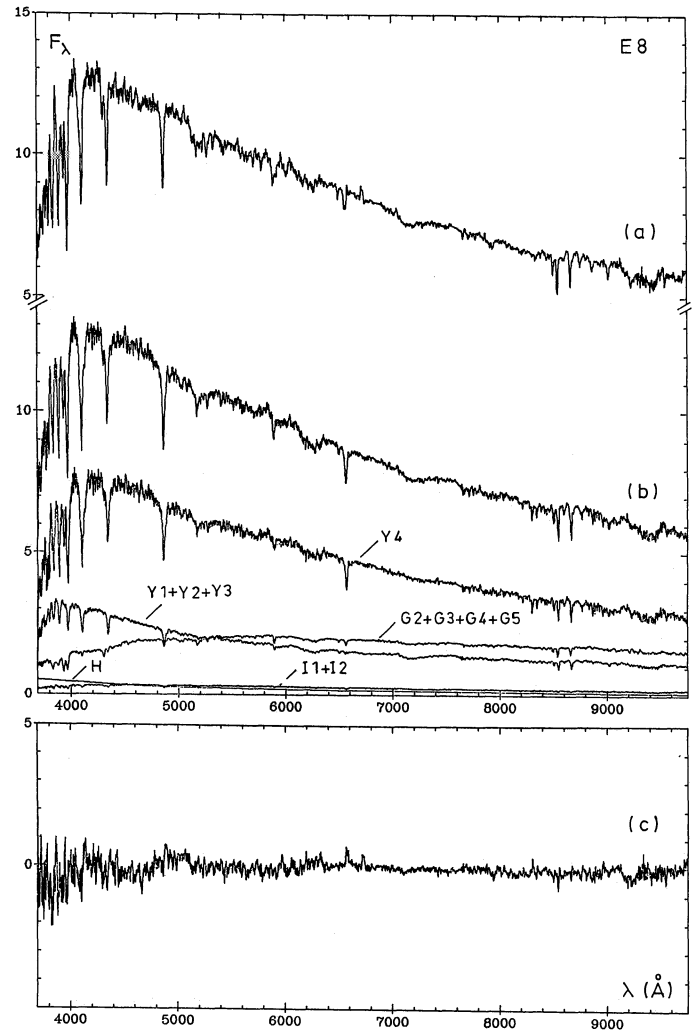
Fig. 8

Fig. 9

this point, high S/N observations of individual galaxies in these groups are required, togehter with the extension of the present method to the near-ultraviolet. However the presence of an intermediate age population in group E 7 is conclusive and further evidence is given by the empirical synthesis in BA 87a. There are also difficulties in the visualization of the results because our intermediate age groups, which are made of Galactic disc and LMC clusters are weak-lined with respect to the expected appearance of SMR intermediate age populations in giant E/S0 galaxies.

Group E 8 which corresponds to the particular case of the low luminosity S0 galaxy NGC 5102, shows a very strong age effect (Table 4h, Fig. 9). There are two methods to compute such strong age effects: (i) using clusters of various ages and metallicites, as decribed in Sect. 3 and (ii) computing the excess population with respect to an underlying red galaxy, which is included together with intermediate and young age clusters in the model. The latter method relies on the assumption that a star burst has occurred indeed. For NGC 5102 both methods lead to the same result. The computations also indicate that the metallicity in NGC 5102 has only reached a sub-solar level, in agreement with its low luminos-

ity. This case represents a major star forming event on top of an underlying population like in group E 4. The bulk of the star burst was formed between the ages 3 to 5 10^8 yr. The fact that this burst is rather old is also suggested by a small H II region continuum contribution and by the residual weak emission lines (Figs. 9b and 9c).

The reddest spiral spectra, in groups S 1 to S 4, are very similar to the red E groups. Groups S 1 to S 4 migrate diagonally in the morphological type vs luminosity class diagram (Table 2). The computations indicate that the maximum metallicity has reached values a factor 4 solar (S 1) to solar (S 4). Their distribution in Table 2 thus implies that the maximum metallicity is related to the bulge luminosity. Note that the most metal poor groups S 3 and S 4 are strong-lined, very different from metal poor globular clusters (BA 87a). Groups S 1 to S 3 do not require a significant contribution from young components, but the small bulges in group S 4 are systematically coupled with a small amount of recent star formation (Table 5d and Fig. 13). This is certainly due to the availability of gas but also to the fact that even a weak star forming event will show up easily with respect to the older population in the small nuclei of low luminosity Sc galaxies.
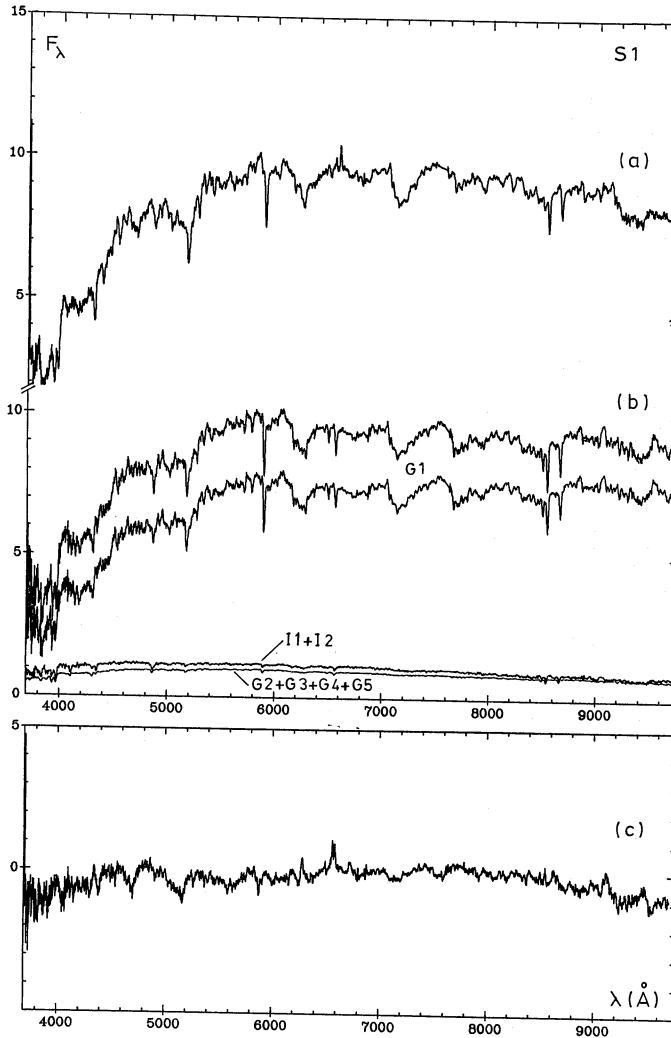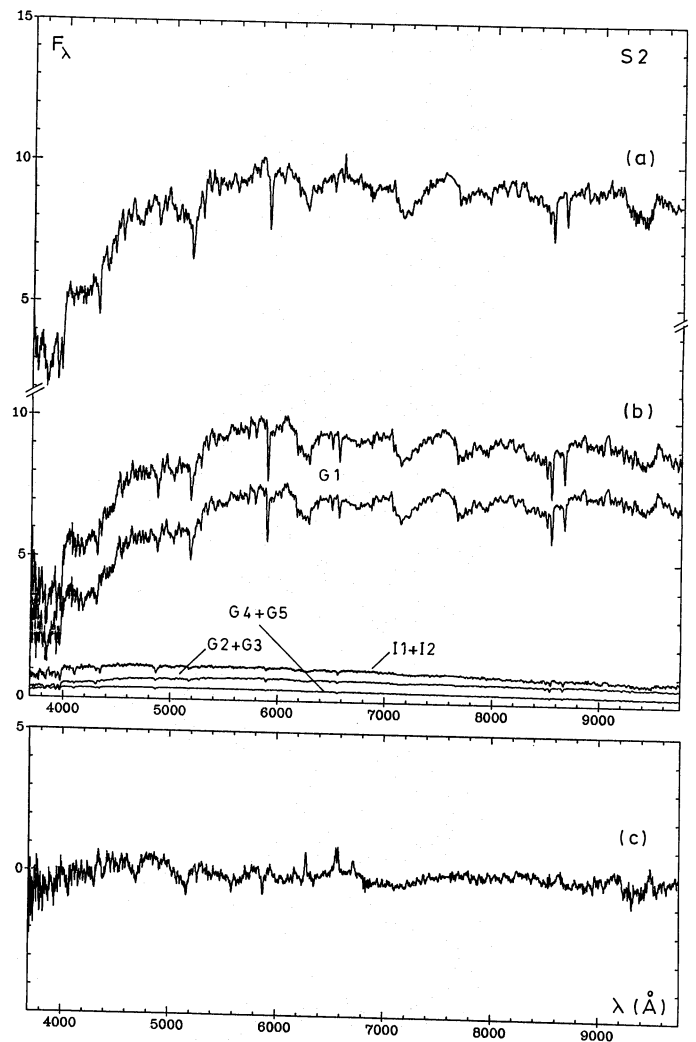
Fig. 10

Fig. 11

In the S 4 group, all galaxies have their Hβ absorption line contaminated by emission. However, some of them have a pure absorption at Hγ and Hδ. So we have used only the latter Balmer lines in the computations. In the groups S 5 to S 7, Balmer lines down to Hδ are emission contaminated, thus the computations rely on metallic features only. The fact that we find a unique family of solutions confirms the powerful use of metallic features, when considered over a wide spectral range, as an age discriminator. An additional test is provided by comparing the computations for the S 4 group, with and without Hγ and Hδ being taken into account, the solution remains the same.

From Figs. 13 to 16, it is possible to estimate directly the relative contribution of younger components at any wavelength. For the bluest group, S 7, the population younger than $3\ 10^8$ yr represents 87% of the flux at 4000 Å and 57% at 9000 Å. This will be an important constraint on the contribution of red supergiants with respect to other red stars in the synthesis using stellar libraries.

For the group S 6 no spectrum was taken for $\lambda > 8000$ Å. However from 6000 to 8000 Å, the spectrum in group S 6 perfectly matches that observed for group S 5. Thus we have used in the

computations for group S 6, the values of W(Ca II) 8542, 8662 Å obtained from the spectrum representative of group S 5. Indeed group S 6 seems to differ from group S 5 only by the presence of a more important young age component (Figs. 14 and 15).

As for group E 8, the S 5 to S 7 groups have been computed with and without an input underlying red galaxy, and the results are essentially the same. The underlying red populations from groups S 3 and S 4 provide the best results, as expected from the distribution observed for groups S 5 to S 7 in Table 2. This indicates that the blue spirals have reached at least the solar metallicity.

The H II region continuum contribution increases steadily from group S 4 to group S 7, in agreement with the strengthening of the emission lines. Indeed, groups S 5 to S 7 include many nuclei which have been spatially resolved into H II regions such as NGC 2903, 2997, 3351, 4303, 4321, 5236, 5248, and 7552 (Sersic and Pastoriza, 1965; Pastoriza, 1975). The contributions of the nuclear H II regions in Table 5 should be regarded as preliminary, because a precise determination requires observations in the near-ultraviolet, where it is more conspicuous. However, we can discuss their average properties, using group S 7, where the H II contri-
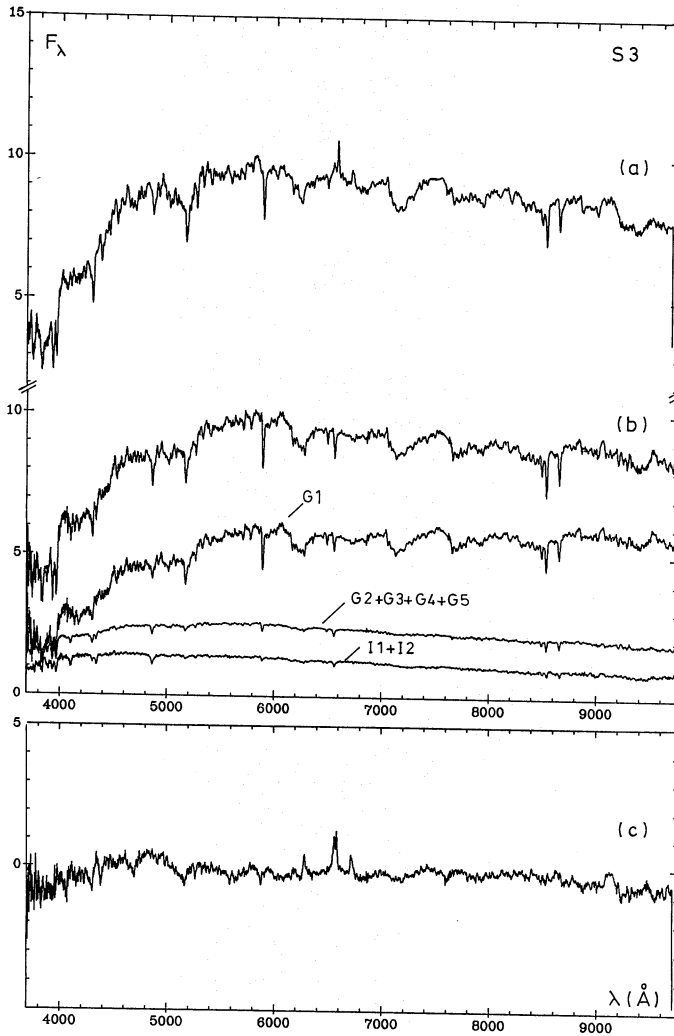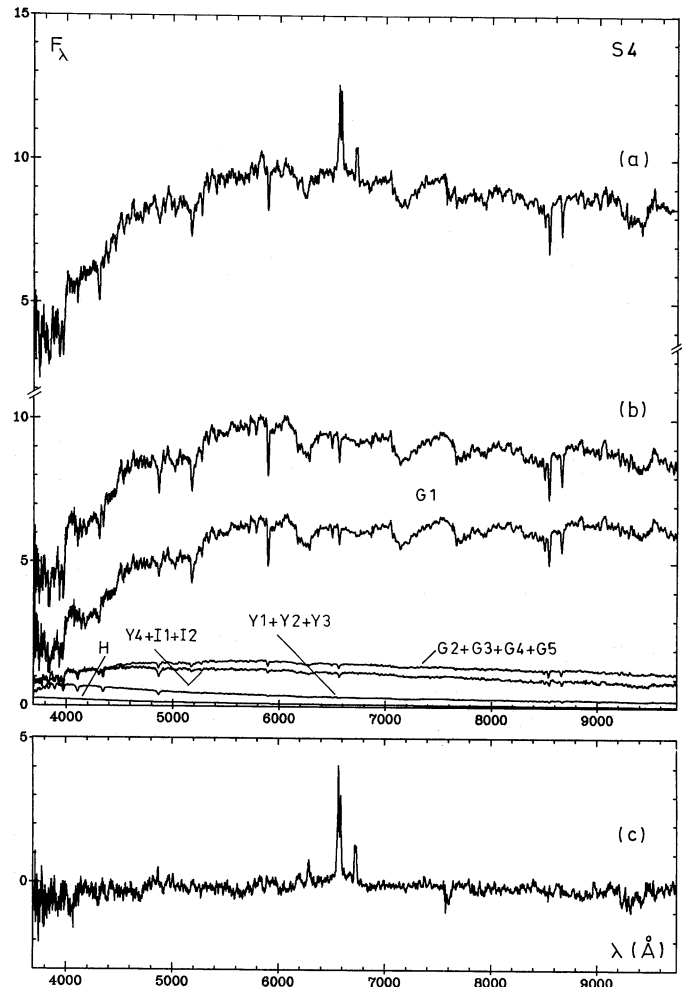
Fig. 12

Fig. 13

bution is the strongest. Adding the featureless H II region continuum (Fig. 16b) with the residuals containing the emission lines (Fig. 16c), we derive $W(H\beta) = 52$ Å, $I([O\,III](4959 + 5007))/I(H\beta) = 0.6$ and $I(H\alpha)/I(H\beta) = 4.2$. It is known that $W(H\beta)$ and the ratio $([O\,III])/I(H\beta)$ are good age indicators (Dottori and Bica, 1981; Copetti et al., 1986). The observed values in our case imply that the average age of the nuclear H II regions is 4.5–$6\ 10^6$ yr. The observed ratio $I(H\alpha)/I(H\beta)$ suggests an internal reddening $E(B-V) = 0.35$. As already pointed out, this high reddening is inherent to star forming regions and does not necessarily apply to the surrounding older populations.

A quantitative comparison of the present results with previous syntheses is difficult because we derive star cluster contributions of various ages and metallicities while previous results were expressed in terms of stellar group contributions of various spectral types and luminosity classes. However, it is gratifying that, at least qualitatively, both approaches agree well in most of their predictions. The synthesis by O'Connell (1976) indicates that in giant elliptical galaxies the bulk of the stars were formed 8 to 11 Gyr ago, with some residual star formation until 4 Gyr ago. This is in fair agreement with our results for this galaxy group.

Pickles (1985) derived turnoff ages of 6 to 10 Gyr for elliptical galaxies of all luminosities. We also find evidence that the E/S0 galaxies in the whole luminosity range have formed stars to look back times of 5 Gyr, but the present method indicates in addition that the rate of star formation must have decreased by a factor 10 sometime between 10 and 5 Gyr. According to the present study, the maximum metallicity reached at a given E/S0 luminosity is in good agreement with Pickles' results for the Fornax elliptical galaxies, considering that he derives mean metallicities. A dispersion of metallicity, as we have detected in E/S0 nuclei, is also predicted by evolutionary synthesis methods (Arimoto and Yoshii, 1987), at least for the total galaxy. The presence of a metal poor component in the nucleus is expected from simple models of galactic chemical enrichment and is also detected by the spectral index method of Rose (1985). However, as pointed out in Sect. 4, a detailed comparison of the metal poor contributions in Table 4 with chemical evolution models requires model predictions for the metallicity distribution in galaxy shells, as well as the consideration of slit projection effects.

Our detection of different amounts of younger age components for the spiral groups is in agreement with the synthesis
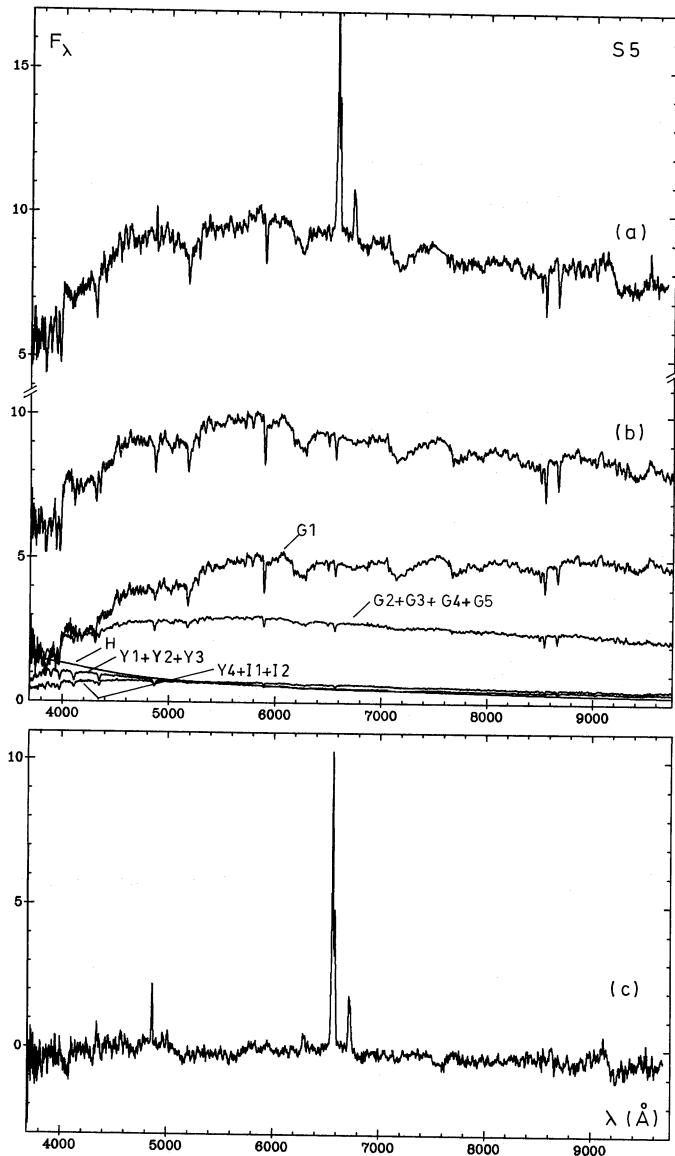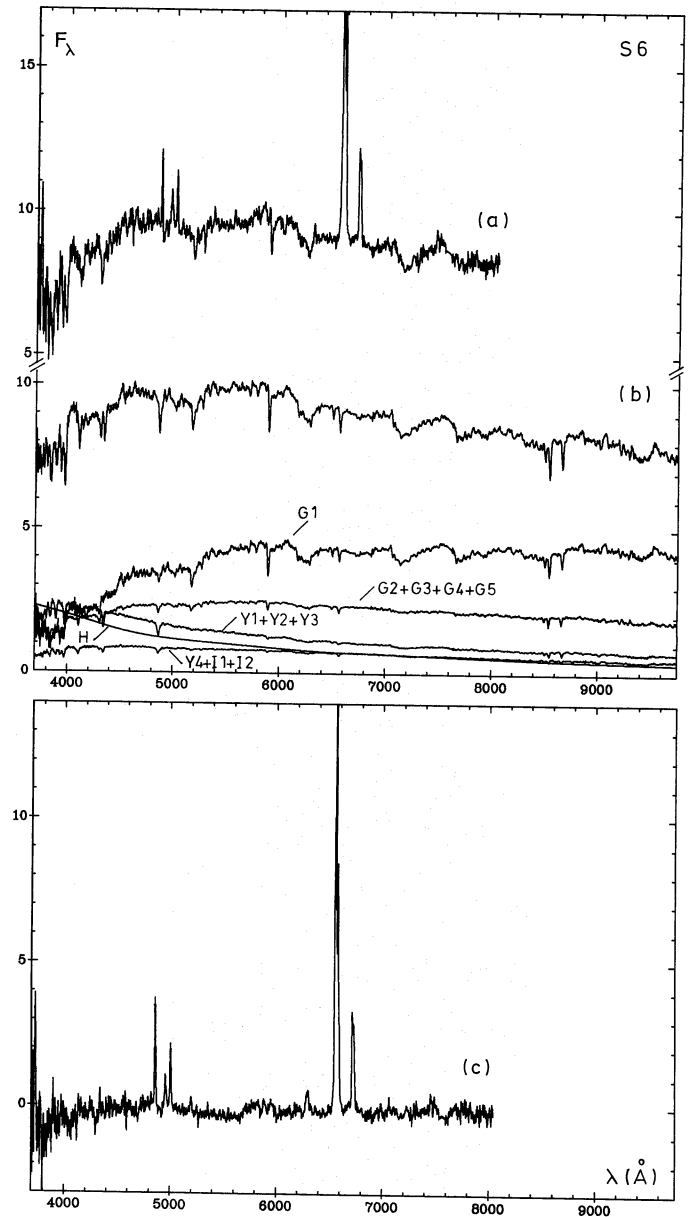
Fig. 14

Fig. 15

results from Turnrose (1976). Also his internal reddening estimates for spiral galaxies, in the range $E(B-V)$ 0.10 to 0.40, are basically compatible with ours. The way we decompose the internal reddening in terms of (i) inclination effects, (ii) global nuclear and bulge absorption, and (iii) absorption inherent to star forming regions, has however given more insight into this problem.

We conclude that synthesis methods based on stellar libraries and the present method are complementary. Both techniques should be further developed and applied to the study of particular objects. Of fundamental importance will also be the application of stellar library methods to the integrated spectra of star clusters, particularly with the help of synthetic spectra for metallicity entries which are difficult to observe.

6. Concluding remarks

A new population synthesis method has been developed which makes use exclusively of a library of star clusters. The method has allowed to date successive stellar generations and to determine the chemical enrichment in E/S0 and spiral galaxies. It has provided a direct estimate of the chemical evolution in these nuclei.

The method will have important applications for distant galaxies. A larger volume can be observed for distant early type galaxies, thus giving information on the global chemical evolution. Also it will be interesting to explore the disc contributions in spirals. For very large redshift galaxies, the method can be used to study galaxies in early evolutionary stages, which are becoming accessible with modern detectors and large telescopes.
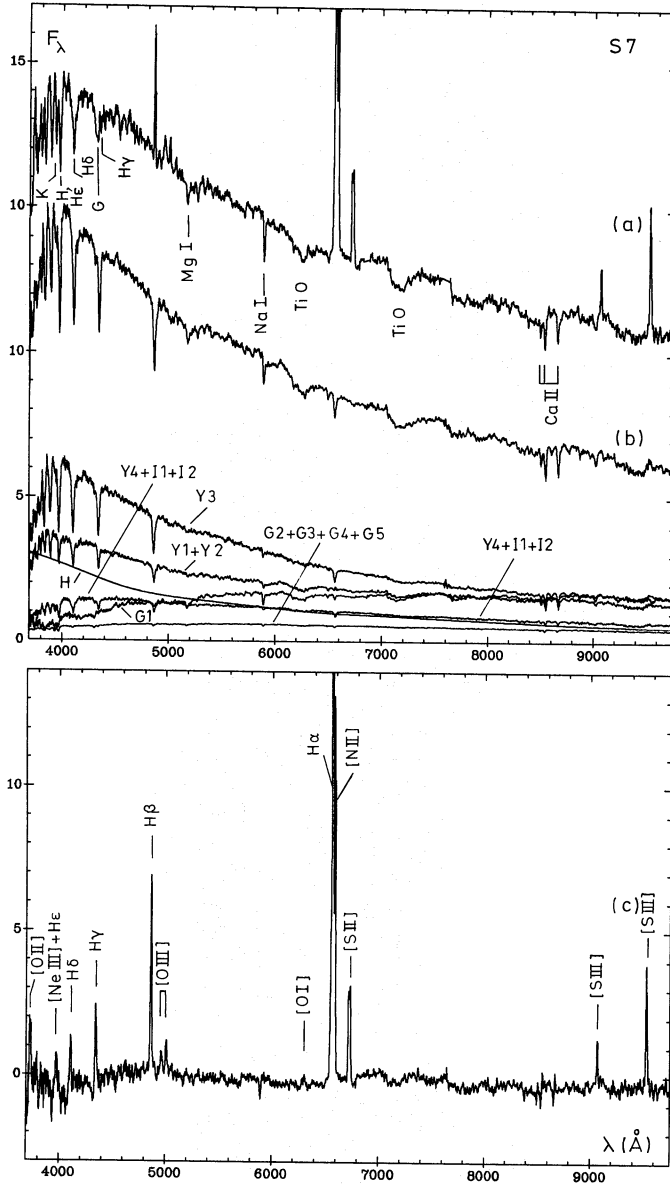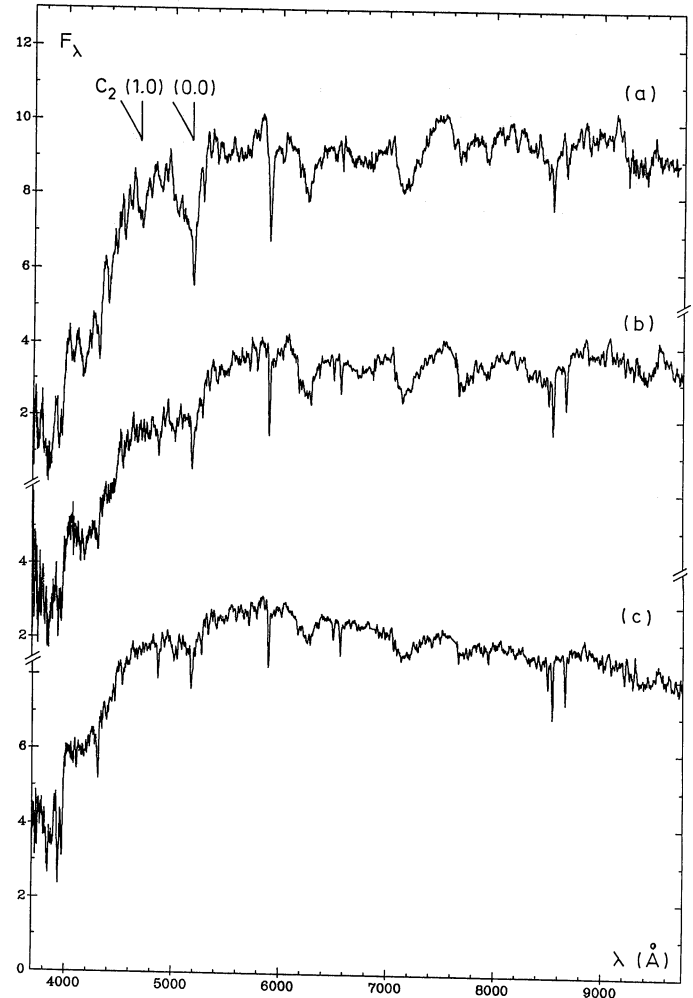
Fig. 16

Fig. 17. a the predicted spectrum for a globular cluster at $[Z/Z_\odot] = +0.6$; **b** and **c** observed globular clusters at respectively $[Z/Z_\odot] = +0.05$ and -0.4

An extension to the ultraviolet range will help to determine more precisely the contributions from hot populations. A preliminary study in this direction is presented in Bica and Alloin (1987d).

Finally, the grid of star cluster properties can be refined with a larger number of cluster observations, particularly for young and intermediate age objects in the Magellanic Clouds, Galactic disc and in M 31. Also of great help will be the use of synthetic spectra.

The present method is complementary to those using a library of stellar spectra. Further development of both techniques will certainly clarify many aspects in the interpretation of integrated spectra.

References

Arimoto, N., Yoshii, Y.: 1987, *Astron. Astrophys.* **173**, 23
Bica, E., Alloin, D.: 1986a, *Astron. Astrophys.* **162**, 21
Bica, E., Alloin, D.: 1986b, *Astron. Astrophys. Suppl. Ser.* **66**, 171
Bica, E., Alloin, D.: 1986c, *Astron. Astrophys.* **166**, 83
Bica, E., Alloin, D.: 1987a, *Astron. Astrophys. Suppl. Ser.* **70**, 281

Bica, E., Alloin, D.: 1987b, *Astron. Astrophys.* **186**, 49

Bica, E., Alloin, D.: 1987c, *Astron. Astrophys.* **181**, 270

Bica, E., Alloin, D.: 1987d, *Astron. Astrophys.* (in press)

Burstein, D., Heiles, C.: 1984, *Astrophys. J. Suppl. Ser.* **54**, 33

Copetti, M., Pastoriza, M., Dottori, H., 1986, *Astron. Astrophys.* **156**, 111

Dottori, H., Bica, E.: 1981, *Astron. Astrophys.* **102**, 245

Hartwick, F.: 1976, *Astrophys. J.* **209**, 418

Humason, M., Mayall, N., Sandage, A.: 1956, *Astron. J.* **61**, 97

Keel, W.: 1983, *Astrophys. J.* **269**, 466

McClure, R., VandenBerg, D., Smith, G., Fahlman, G., Richer, H., Hesser, J., Harris, W., Stetson, P., Bell, R.: 1986, *Astrophys. J.* **307**, L49

O'Connell, R.: 1976, *Astrophys. J.* **206**, 370

Pagel, B., Edmunds, M.: 1981, *Ann. Rev. Astron. Astrophys.* **19**, 77

Pastoriza, M.: 1975, *Astrophys. Space. Sci.* **33**, 173

Pickles, A.: 1985, *Astrophys. J.* **296**, 340

Rose, J.: 1985, *Astron. J.* **90**, 1927

Sandage, A., Tammann, G.: 1981, A revised Shapley-Ames Catalogue of Bright Galaxies, Carnegie Institution of Washington

Scalo, J.: 1986, in *Luminous Stars and Associations in Galaxies*, ed. C. de Loore et al., p. 451

Sersic, J., Pastoriza, M.: 1965, *Publ. Astron. Soc. Pacific* **77**, 287

Sparks, W., Wall, J., Thorne, D., Jorden, P., van Breda, I., Rudd, P., Jorgensen, H.: 1985, *Monthly Notices Roy. Astron. Soc.* **217**, 87

Sparks, W., Ellis, R., McMahon, R., Terlevich, R., Melnick, J.: 1987, *Monthly Notices Roy. Astron. Soc.* **225**, 769

Turnrose, B.: 1976, *Astrophys. J.* **210**, 33